A Complete Software-Based IF GNSS Signal Generator for Software Receiver Development

Olivier Julien, Bo Zheng, Lei Dong, and Gérard Lachapelle
Position, Location and Navigation (PLAN) Group
(http://plan.geomatics.ucalgary.ca)
Department of Geomatics Engineering
University of Calgary

BIOGRAPHIES

Olivier Julien is a Ph.D. candidate in the above department. In 2001, he graduated from ENAC (French University for Civil Aviation), Toulouse, France, as an electrical engineer, majoring in digital communications. His research includes GPS/Galileo interoperability as well as GNSS receiver design.

Bo Zheng is a Ph.D. student in the same department. He received his B.S. (1996) in Electronics Engineering at Northwestern Polytechnical University, China, and his M.Sc. (1999) in Electronics Engineering from the Chinese Academy of Space Technology. His current research interests are GPS receiver software technology and GPS signal simulation.

Lei Dong is a research associate in the same department. She received her B.S. (1992) in industry automatic control and M.S. (1995) in Electronics Engineering at Northwestern Polytechnical University (Xi'an, China). Se received her second M.S. (2004) in Geomatics Engineering at the University of Calgary. Her current research focuses on GPS receiver technology and GPS signal simulation.

Dr. Gérard Lachapelle holds a CRC/iCORE Chair in Wireless Location in the Department of Geomatics Engineering. He has been involved with GPS developments and applications since 1980 and has authored/co-authored numerous related publications and software. More information is available on http://plan.geomatics.ucalgary.ca

ABSTRACT

The recent development of Global Navigation Satellite Systems (GNSS) software receivers has brought a new perspective to receiver design. The first step necessary to use them is to have access to sampled data at an Intermediate Frequency (IF). These sampled data can be provided through two different ways. First, an RF front-end that would sample data coming from either the real satellites or from a hardware signal generator, if the latter exists at all for the signals of interest. Real data might not be suitable when a specific aspect of GNSS is studied, especially in a research and development context, or might not yet be available as in the case of GPS L5 and Galileo signals. Hardware signal simulators were created to fill that gap, and are now widely used. However, they are very expensive, may not be available for the signals of interest and consequently might not be always suitable for specialized research due to their lack of flexibility. Sampled data can also be provided by a software IF signal generator. Such a tool includes signal simulation as well as front-end filtering and sampling, fully software-based, and can fed directly into a software receiver. Such programs are already used and are often created by the research groups themselves to fit their research programs. Although they offer a total control of all the parameters for simulation purpose, they are often highly specialized and, as such tend to model only a part of the error sources of interest, e.g., jamming or multipath.

The Position, Location And Navigation (PLAN) research group of the Department of Geomatics Engineering has developed a complete IF signal generator that can model the new GPS and Galileo signals propagation channels while being versatile and customizable. This signal generator allows for the modeling of pre-defined environments for specific applications. It offers a direct access to IF sampled data that can be directly used by a software receiver. From an ephemeris file, an entire constellation of satellites can be easily simulated. The entire GNSS propagation channel is then modeled. Finally, the front-end filter and the Analog-to-Digital Converter (ADC) (1-bit quantization) are simulated. A first Matlab/C, GPS-only version of this IF signal generator modeled thermal noise, satellite clock errors, atmospheric errors, the front-end filter, and an ADC. The current enhanced version, written in C++ to improve processing speed, now includes multipath modeling,

different antenna gain patterns, and multiple signal waveform generation. These were all implemented in a modular manner in order to be easily modified or enhanced by new models or algorithms for further applications.

The multipath channel is critical because different applications require different multipath models. It has been divided in two main components: diffuse and specular reflections. This allows for a versatile and easily reconfigurable environment. The antenna gain pattern also plays a significant role for many applications. Finally, the simulator includes a signal waveform module where the user can either create its own signal waveform (for instance candidates for Galileo signals) or select one from pre-defined signals (for instance L1, L5). This allows for testing in a simulated environment of new signals that are not broadcast yet. Finally, the user trajectory can be easily defined, and static or kinematic scenarios can be simulated.

As a result, this complete IF signal generator is very well suited for the development phase of a software receiver due to its versatility. It also allows for a wide range of thorough tests, including the impact of atmospheric biases, the study of tracking loops in different conditions, and the assessment of multipath impact in a pre-defined environment. The full access to the sampling frequency value, front-end filter definition or ADC parameters also offers a great opportunity for cost-effective detailed studies of tracking loops and error mitigation techniques at the receiver level. Sources of interference can be easily added to the program to simulate specific environments. This software signal generator can also be used to feed a multi-frequency multi-system software receiver for the prototyping of a combined GPS/Galileo receiver.

INTRODUCTION

In a quest for flexibility and versatility, more and more research groups are developing Global Navigation Satellite Systems (GNSS) software-based receivers. Having a full access to the 'black box' have raised the possibility to control totally the reception and the processing of the GNSS signals according to needs, offering the possibility to reconfigure the receiver depending on the kind of situation one may face.

However, the development of a GNSS software receiver is a long and difficult task, as it requires long and thorough testing. Having a robust and efficient platform to test an implementation provides a significant gain in time. In that perspective, the PLAN group decided to develop a software GNSS IF signal simulator, as flexible as possible, that would provide simple to complex environment to test the development and/or testing of different receiver technologies using its newly developed software receiver (Ma et al 2004).

The use of a hardware signal generator has many advantages, but at a very high cost. Moreover, it has to be combined with a front-end that might not be suitable for software receivers. A software-based IF signal generator offers the freedom to many researchers in a same group to test their own receiver developments without having to time share a hardware simulator. It also offers the possibility to test different signal modulations that might not be available yet in hardware. Finally it has the great advantage to be very flexible and to allow the design of precise settings for testing in particular environments. The GNSS IF signal simulator presented in this paper does not pretend to be thoroughly suitable for all applications, but it was designed to be an efficient tool to assist researchers in a cost effective manner.

The first part of this study will summarize the development previously realized of a GPS IF signal simulator [Dong 2003, Dong et al 2004]. Because it has been demonstrated in that first phase that the model used led to correct 3-D positioning, this paper will focus on the measurement domain more than on the position domain in the following sections. The second part will focus on the different new signals that can now be simulated, transforming the GPS IF simulator into a full GNSS IF simulator. Finally, the third part will focus on the enhancements that were brought on the simulation of the different sources of errors, and the modeling of some front-end hardware components such as the antenna or the received power pattern.

INITIAL GPS IF SOFTWARE SIMULATOR

The first version of the IF software receiver was designed to simulate GPS C/A signal only. It was done jointly with the realization of a GPS software receiver [Dong et al 2004, Ma et al 2004]. For that matter, a thorough modeling of the received signal and each individual error had to be investigated. Although all the details are given in [Dong 2003], this section will summarize the main results of this investigation. The overall IF GPS simulator structure is given in Figure 1.

The GPS constellation is loaded using a broadcast ephemeris file that can be downloaded from the Crustal Dynamics Data Information System institute (CDDIS) website, as an example. It allows the simulation of a true GPS constellation at a given time. Moreover, the ephemeris data allows taking into account relativistic effects. The computation of the satellite position also allows disregarding the satellites situated below the horizon, or under a specified elevation mask.

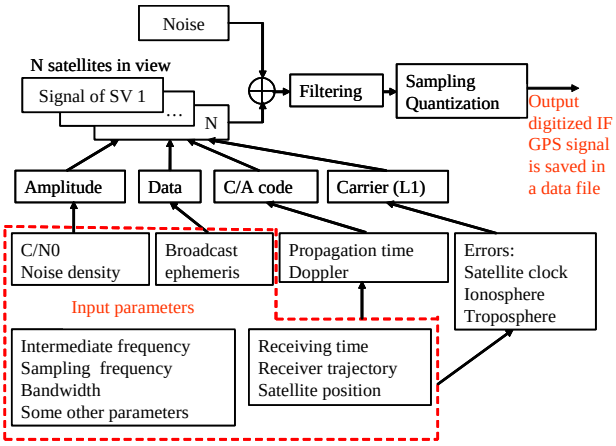

Figure 1 – Initial IF GPS Simulator Structure [Dong et al 2004]

Once the satellites in view are selected and their positions computed, the signal coming from each satellite has to be modeled. The model used in the GPS IF signal generator is

$$S_{IF}(t) = \sqrt{2P}D\left(t - T_d - \delta t_{Iono}^{L1}\right)C\left(t - T_d - \delta t_{Iono}^{L1}\right) \cos\left(\omega_{IF}t - \omega_{L1}\left(T_d - {}^{L1}_{Iono}\right) + \varphi_0\right) + Noise + MP \quad (1)$$

with

$$T_d = \delta t_{SV} + \delta t_{eph} + \delta t_{Tropo} + t_p \quad (2)$$

where

t	is the signal receiving time
P	is the received signal power
D	is the navigation data message
C	is the spreading code
f_{IF}	is the IF frequency
f_{L1}	is the L1 frequency
φ_0	is the Initial phase
MP	represents multipath
δt_{Iono}	is the delay due to ionosphere
δt_{Tropo}	is the delay due to troposphere
δt_{SV}	is the satellite clock error
δt_{eph}	is the ephemeris error
t_p	is the propagation delay

Although part of the final tracking error, the receiver clock error cannot be, a priori, included in the IF signal model, as it is an error source happening during tracking (from the NCO). This will be investigated in further details in the third section.

It should also be noticed that equation (1) includes the Doppler information through the term $\omega_{L1}\left(T_d - \delta t_{Iono}^{L1}\right)$.

Because the signal takes some time to travel from the satellite to the receiver antenna, the Earth's rotation has to be taken into account. Indeed, the IF GPS simulator uses the receiving time as its reference time. This means that the satellite position at the time of the transmission has to be calculated in order to model the correct range. This is implemented in the receiver architecture.

The ionosphere error model is adapted from the ionosphere error model used in SimGNSSII™, a software package developed by the University of Calgary that can model GNSS measurements. It has been used extensively for carrier phase positioning research [e.g., Alves 2001, Julien et al 2004a, b] as well as for GPS/Galileo reliability testing [Kuusniemi et al 2004].

The satellite clock error was modeled through the three parameters sent by each satellite in the ephemeris data. The thermal noise was added taking into account the front-end filter shape. Each satellite C/N_o could be set individually, allowing testing with different received signal power. One bit quantization was possible after filtering, as most of the hardware receivers use this quantization.

A GPS software receiver was used in order to validate each step of the IF simulator realization. A series of test comparing the IF simulator data against IF data obtained from the combination of a GPS hardware generator and a L1 front-end were done. The corroborating results showed that a correct implementation of the GPS IF signal simulator was successfully achieved.

Because these tests were conducted in the position domain and were conclusive, they proved that the IF signal model as well as the constellation generation module was successfully implemented. Consequently, the enhancement of this version focuses on the measurement domain. The following starts with the description of the implementation of new signal waveforms, namely GPS L5 and BOC modulation. A description of the signal model enhancement will then be presented.

SIGNAL WAVEFORM MODEL

The signal waveform module can create two signals already fully defined, GPS L1 C/A and GPS L5, as well as some candidates for the Galileo signals, such as BOC(1, 1). These signals can be output either separately or in a combination mode. For example, both L5 and Galileo signals can be output simultaneously to feed a multi-frequency multi-system software receiver for the prototyping of a combined GPS/Galileo receiver.

The mathematical model of the IF GPS L1 C/A signal has already been given earlier. As to the IF GPS L5 signal, it can be represented by the following equation, including all the propagation errors simulated in the signal generator:

$$S_{IF}^{L5,i}(t) = \sqrt{P_{L5}^{i}} \cdot D_{L5}^{i}\left(t - T_d^i - \delta t_{Iono}^{L5,i}\right) \cdot NH_{10}\left(t - T_d^i - \delta t_{Iono}^{L5}\right) \cdot C_{L5\_I}^{i}\left(t - T_d^i - \delta t_{Iono}^{L5}\right) \cdot \cos\left(\omega_{IF} t - \omega_{L5}(T_d^i - \delta t_{Iono}^{L5}) + \varphi_0^i\right) + \sqrt{P_{L5}^{i}} \cdot NH_{20}\left(t - T_d^i - \delta t_{Iono}^{L5}\right) \cdot C_{L5\_Q}^{i}\left(t - T_d^i - \delta t_{Iono}^{L5}\right) \cdot \sin\left(\omega_{IF} t - \omega_{L5}(T_d^i - \delta t_{Iono}^{L5}) + \varphi_0^i\right) \quad (3)$$

where

$S_{IF}^{L5,i}$	is the IF L5 signal for SV_i
D_{L5}	is the navigation data bits for SV_i
NH_{10}	is the 10 bit Neumann-Hoffman code
NH_{20}	is the 20 bit Neumann-Hoffman code
$C_{L5\_I}^{i}$	is the in-phase L5 PRN code for SV_i
$C_{L5\_Q}^{i}$	is the quadrature-phase L5 PRN code for SV_i
ω_{L5}	is the L5 carrier angular frequency
$\delta t_{Iono}^{L5,i}$	is the ionosphere bias at L5 for SV_i

The GPS L5 spreading code length is 10,230 chips and its chipping rate is 10.23 MHz. It possesses an in-phase (containing navigation data) and quadrature-phase (without navigation data) component. Each component carries half of the total signal power. Thus, a tracking scheme using only the dataless (i.e. pilot) channel for instance will use only half of the total signal power. However, the availability of the pilot channel will allow a coherent carrier tracking that will make the receiver more robust to low C/N_o [Tran and Hegarty 2002, Macabiau et al, 2003] and will allow for better acquisition performance [Bastide et al 2002; Hegarty et al 2003]. Finally, the GPS L5 signals will use Neumann-Hoffman (NH) encoding. These codes are short codes with a low bit rate. A NH code of 10 bits is used on the data channel, and a NH code of 20 bits is used on the pilot channel. Their bit length is equal to one full spreading code length, or 1 ms. Although they complicate the acquisition procedure [Zheng & Lachapelle 2004, Macabiau et al 2003; Hegarty et al 2003], they are intended to help mitigating narrow-band interference by multiplying the number of spectral lines carrying the signal energy (more spectral lines carrying the same energy means that each spectral line will carry less energy), as it will be explained in the next sub-section.

The output of the signal is the combination of the signals coming from all satellites in view. It can be represented as:

$$S_{IF}^{L5}(t) = \sum_{i=1}^{N}\left(S_{IF}^{L5,i}(t)\right) \quad (4)$$

where

N is the number of GPS satellites in view

The Galileo E1 civil signal is simulated on L1 with the choice of any BOC(n, 1) modulation. L1 C/A-codes are implemented as the spreading codes as no codes have been proposed so far as Galileo spreading codes. Because the Galileo E1 is composed of both in-phase and quadrature-phase components, 74 PRN codes are needed to generate 37 pairs of BOC(n, 1) signal. As only GPS C/A codes are used,, only 17 satellite signals can be generated simultaneously, which is more than enough assuming that less than 17 satellites will be in view at the same time. The only constraint is in the case where the generation of both GPS L1 C/A and Galileo E1 codes is needed, in which case special care has to be taken in order to avoid having two signals using the same spreading code. The possibility to implement new codes is also under investigation.

The mathematical model for the BOC(n, 1) signal for satellite *i* can be represented as follows:

$$S_{IF}^{E1,i}(t) = \sqrt{P_{E1}^{i}} \cdot D_{E1}^{i}\left(t - T_d^i - \delta t_{Iono}^{E1,i}\right) \cdot SC\left(t - T_d^i - \delta t_{Iono}^{E1,i}\right) \cdot C_{E1\_I}^{i}\left(t - T_d^i - \delta t_{Iono}^{E1,i}\right) \cdot \cos\left(\omega_{IF} t - \omega_{L1}(T_d^i - \delta t_{Iono}^{E1,i}) + \varphi_0^i\right) + \sqrt{P_{E1}^{i}} \cdot SC\left(t - T_d^i - \delta t_{Iono}^{E1,i}\right) \cdot C_{E1\_Q}^{i}\left(t - T_d^i - \delta t_{Iono}^{E1,i}\right) \cdot \sin\left(\omega_{IF} t - \omega_{L1}(T_d^i - \delta t_{Iono}^{E1,i}) + \varphi_0^i\right) \quad (5)$$

where

S_{IF}^{E1}	is the IF BOC(n, 1) signal for SV_i
D_{E1}	Navigation data bits for SV_i
SC	Rectangular subcarrier
$C_{E1\_I}^{i}$	In-phase E1 PRN code for SV_i
$C_{E1\_Q}^{i}$	Quadrature-phase E1 PRN code for SV_i

Note that in the latest Galileo E1 civil signal structure, a tiered code (similar concept as the NH codes) will be implemented on each data and dataless channel. Because these codes have not been released yet, they were omitted in the present implementation.

As in the case of GPS L5, the Galileo E1 signals can be represented as:

$$S_{IF}^{i}(t) = \sum_{i=1}^{N}\left(S_{IF}^{E1,i}(t)\right) \quad (6)$$

Verification of the Generated Signals

Three verification schemes are implemented to make sure the newly generated L5 and BOC(n, 1) signals are correct. First, the PRN codes modulated on these two signals are examined. Second, the power spectrum of the simulated signals are plotted and analyzed. Third, by using several acquisition schemes developed in the PLAN group for L5, the acquired Doppler frequency and code delay are compared with the simulated ones.

Since the PRN codes modulated on Galileo BOC(n, 1) signal are C/A codes, which has already been verified in the previous signal generator, only the GPS L5 PRN codes need to be examined. The first 20 bits of the in-phase code of PRN1, for instance, are:

{-1, -1, 1, -1, -1, 1, 1, 1, -1, 1, -1, 1, -1, 1, 1, 1, -1, 1, -1, -1}

For the quadrature phase of PRN1, they are

{-1, -1, 1, 1, -1, -1, 1, 1, -1, 1, -1, -1, 1, 1, -1, 1, -1, -1, 1, 1}

The code balance (the summation of 1s and -1s for the length of the code) is {-2} for the in-phase code and {2} for the quadrature-phase code. These results, also done for the other PRNs, are agreeing with those in [Spilker et al 2001]. Therefore, the PRN codes are shown to be correct.

The GPS L5 power spectral density without the NH codes is shown in Figure 2 at baseband. The main lobe has a sinc envelope and a width of 10.23 MHz as expected. The ratio between the GPS L5 code chipping rate and the code length equals 0.001, meaning that it has spectral rays every 1 KHz. The use of NH codes artificially extends the length of the spreading code by an amount equal to the NH code length (10 and 20 in this case). This results in the presence of spectral rays every 100 Hz for the in-phase component and every 50 Hz for the quadrature-phase channel. As already mentioned, this implies a lowering of the power spectral density level, as more spectral rays carry the same power. This can be seen in Figure 3 and Figure 4, which show the L5 in-phase and L5 quadrature-phase power spectral density, respectively. As a conclusion, the implementation of the NH code is validated.

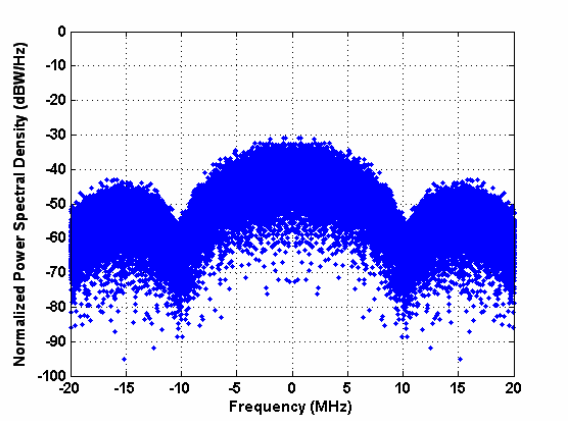

Figure 2 – Power Spectral Density of L5 Signal Without Neumann-Hoffman Code

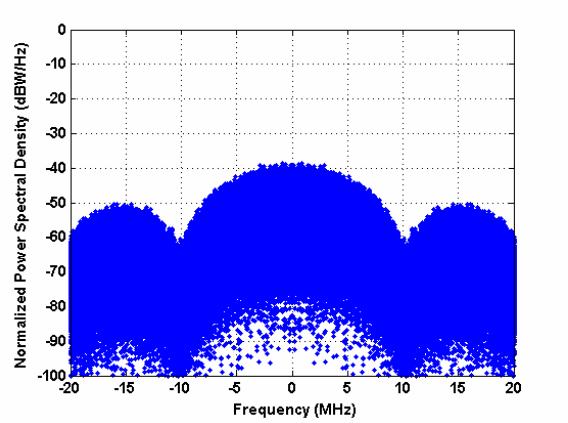

Figure 3 – Power Spectral Density of L5 Signal With NH(10) representing the In-Phase Component

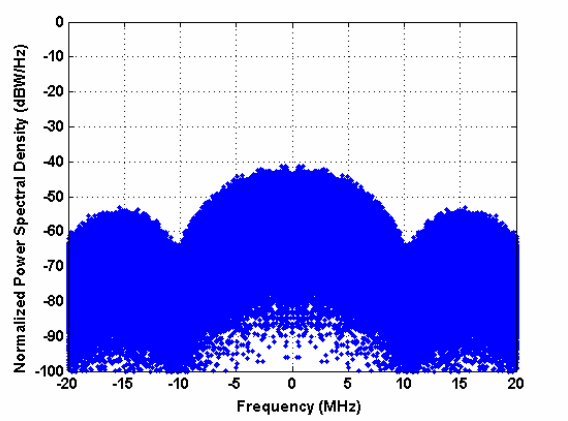

Figure 4 - Power Spectral Density of L5 Signal With NH(20) representing the Quadrature-Phase

In order to test for the BOC(1,1) generated signal, Figure 5 shows its (correct) power spectral density. The power is mainly distributed in the two split spectrum.

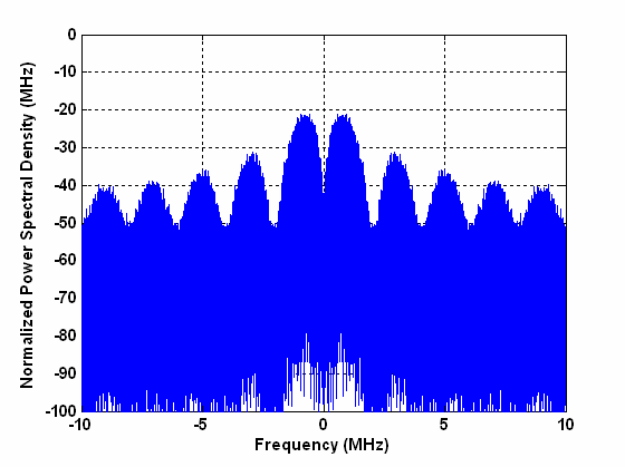

Figure 5 – Power Spectral Density of BOC(1,1) Signal

Finally, the acquisition tests can be analyzed for GPS L5. For this purpose, a 1 ms coherent integration and 10 ms non-coherent integration are implemented to test for the acquisition performance of the L5 signal. The results are shown in Figure 6. The acquired Doppler frequency and code delay are 1000 Hz and 0.354 ms respectively, where the true Doppler and code delay are 1088.23 Hz and 0.354 ms respectively. Since the frequency bin size for 1 ms coherent integration is set to 666.7 Hz, it corresponds to the detection of the correct correlation.

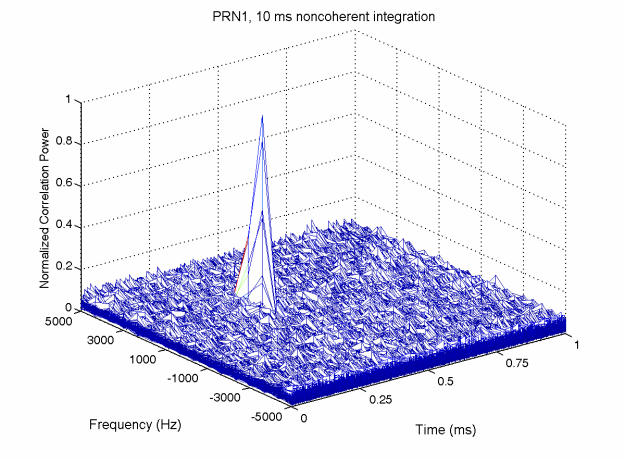

Figure 6 – Acquisition of the L5 Signal using Non-Coherent Integrations

As an example of the use of the new generated signals, another acquisition algorithm for the GPS L5 pilot channel was tested by Zheng & Lachapelle (2004). The main idea of this approach is to eliminate the frequency information of the incoming signal, thus only one dimension search of the initial point of the PRN code is needed in the first step. Acquisition of the Doppler frequency and NH code can be easily performed after the code delay detection. Details of this method can be found in [Zheng & Lachapelle 2004]. Figure 7, obtained using this acquisition scheme, shows that the correct code delay was found.

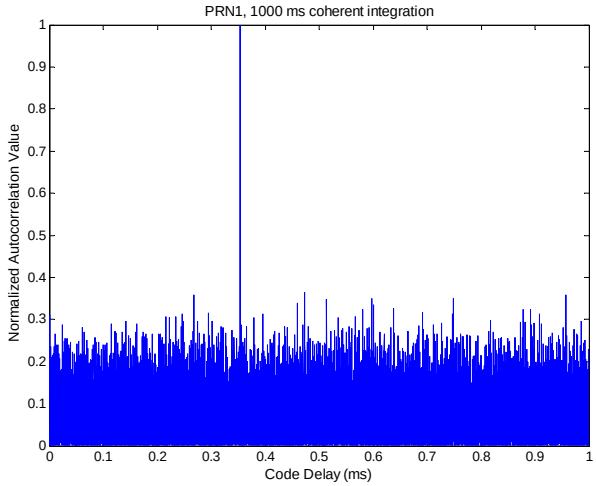

Figure 7 – Acquisition of L5 Signal Using Frequency Removal Method

Now that the GNSS signal generation module has been described, the following section will discuss the signal propagation channel and the improvement in the error models brought by the second version of the GNSS IF signal generator.

ENHANCED PROPAGATION CHANNEL MODEL

Two different types of improvement will be described herein: (1) the error modeling, and (2) the antenna modeling. The error modeling deals with the multipath and satellite oscillator error. The antenna modeling deals with the effect of the satellite and receiver antennas on the received signal.

Satellite Oscillator Model

The satellite oscillator error originates from the fact that the oscillator does not remain exactly at its nominal frequency. It contains a frequency noise whose power spectral density can be modeled as [Winkel 2003]:

$$S_{Osc\_Err}(f) = \frac{h_{-2}}{2f^2} + \frac{h_{-1}}{2f} + \frac{h_0}{2} \qquad (7)$$

where h_{-2}, h_{-1}, h_0 represent the random walk, Flicker and white components of the oscillator frequency error.

The frequency error translates into a phase offset that will impair the proper transmission of the signal. Different oscillators will experience different frequency errors. The resulting timing error is usually represented through the Allan variance, which represents half of the root mean square of the timing error between two adjacent samples separated by a true time interval τ. The three components of the oscillator frequency noise will have a different

effect on the Allan variance. The Allan variance of an oscillator is [Winkel 2003]:

$$\sigma_A^2(\tau) = \frac{h_0}{2\tau} + 2\ln(2)h_{-1} + \frac{2\pi^2}{3}\tau h_{-2} \qquad (8)$$

The oscillators used in satellites are either Rubidium or Cesium. Winkel (2003) proposed a method to generate the phase error based on a system of differential equations. It offers a very practical way to generate such an error source with very small deviations from the Allan variance, as shown in Figure 8.

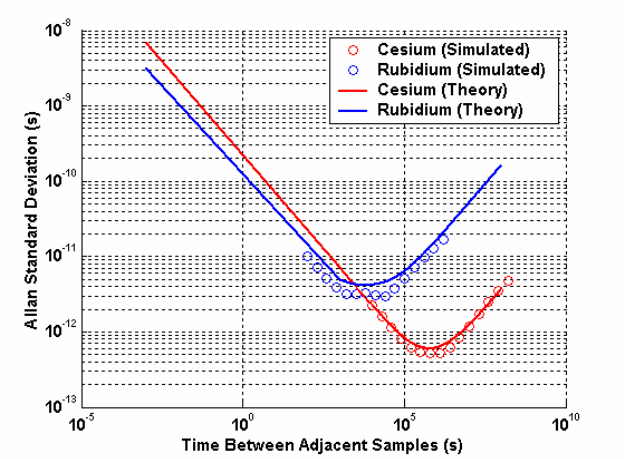

Figure 8 – Theoretical and Simulated Allan Standard Deviation for Standard Cesium and Rubidium Oscillators

Figure 9 shows the behaviour of the simulated Cesium and Rubidium oscillator phase error over 4 hours. It can be seen that the induced phase error is varying very slowly and is minimal in the overall error budget. As a result, it will not result in a significant difference in the final tracking result.

However, one of the objectives with modeling the oscillator phase error was the possibility to model the receiver phase error as well due to the inverse problem:

$$\underbrace{\cos(\omega_{IF}t - \omega_{Osc}\tau_{Rx})}_{Incoming}\underbrace{\cos(\omega_{IF}t)}_{Local} = \underbrace{\cos(\omega_{IF}t)}_{Incoming}\underbrace{\cos(\omega_{IF}t - \omega_{Osc}\tau_{Rx})}_{Local} \qquad (9)$$

where

ω_{Osc} is the oscillator base pulsation

τ_{Rx} is the time error due to the oscillator frequency noise

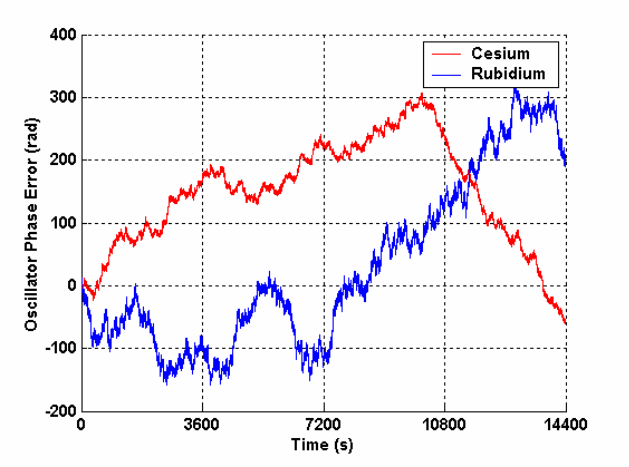

Figure 9 – Example of Cesium and Rubidium Oscillator Phase Error over 4 Hours

However, equation (9) does not take into account the effect of the filter front end, neither the quantization. A narrow filter will surely change the phase error, as it will modify the short term variation, and remove most of the white noise component of the frequency error. A wide filter could only slightly change the phase error, but this could be enough to modify its Allan variance. If quantization is used, it will affect the phase error and it might not represent the effect of the receiver clock error. However, modeling a 'low-cost' satellite oscillator (Quartz or TCXO for instance) can be used to model very short and sudden changes in the signal's dynamics in order to test a software receiver.

Multipath Modeling

The objective for modeling multipath was to enable the testing of multipath mitigation techniques in a fairly realistic environment. Many studies have been done to characterize multipath in different environments [Jahn et al 1996, Brenner et al 1998, Dottling et al 2001, Steingrass et al 2004]. They all underline that the multipath in the signal propagation channel, when using a spread spectrum technique can be divided in near and far echoes. Near echoes usually have a low power, and their power decrease exponentially with their delay. They are scattered multipath. Far echoes have longer delays, and their power is a function of the reflective surface(s). These two types of multipath were intended to be modeled.

Near Echoes

Because this GNSS IF simulator is intended to simulate real data, it was decided to try to model each type of error as close as possible from the truth. As a result, although stochastic models about the impact of multipath on the direct signal exist [Ma et al 2001], it was decided to model all scattered multipath entirely at the IF level. One

way to realize this was discussed by Brenner et al (2003), and used by Hegarty et al (2004). It consists in modeling 500 small reflectors randomly located in a 100-m circle around the antenna.

The mean power of each near echo can be modeled as [Jahn et al 1996]:

$$P_{ne}(d) = P_0 e^{-\alpha d} \tag{10}$$

where

P_0	is the average maximum power received from near echoes
d	is the delay of the echo
α	represents the decay of the echo power with its delay

The amplitude a of the echo varies around its mean value following a Rayleigh distribution:

$$P_{Rayleigh}(a) = \frac{a}{\sigma^2} e^{-\frac{a^2}{2\sigma^2}} \tag{11}$$

with

$$2\sigma^2 = P_{ne}(d) \tag{12}$$

Different environments can then be modeled by changing the decay of the received power and the reflector's distance from the antenna. An example of such model is shown in Figure 10 for a P_0 of -16.5 dB and an α of -5 dB/ms. This approach is very suitable for this application and has been tested successfully for the software receiver. However, when high sampling frequencies are used, it brings a huge computational burden that might make the simulation inoperable, as for each reflector, the delay and power have to be adjusted with each sample. As a consequence, this tool can be used with signals with relatively small bandwidths and using a narrow filter, typically around a sampling frequency of 5 MHz. For larger sampling frequency, a lower number of small reflectors have to be simulated in order to have a decent computation time.

The opportunity to simulate this kind of multipath is very suitable for dedicated environment where any source of error has to be modeled. It can also be used as another source of strong multipath, when testing an algorithm in harsh environments, with the possibility to increase the power of each echo signal.

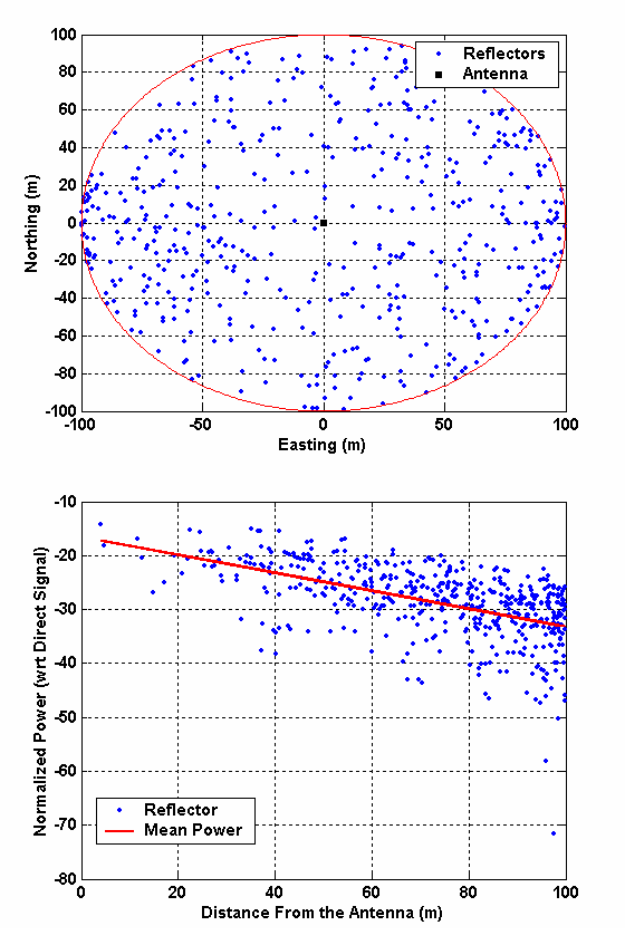

Figure 10 – Repartition (Top), and Normalized Power of 500 Small Reflectors in a 100 Metre Circle around the User.

Far Echoes

Far echoes should be modeled differently from near echoes due to their different nature. They originate from larger and smoother surfaces and can have a stronger power depending upon the reflective surfaces. Two sources of specular reflections were modeled for the IF GNSS signal simulator, namely the ground and obstacles.

Ground reflections are processed separately. An infinite horizontal ground was assumed, and a dedicated reflection coefficient can be input according to the surface simulated. Because the ground is assumed flat and smooth, it is possible to apply Snell' laws for reflection: where the incident angle is equal to the reflection angle. Knowing where the satellite is at all times from the ephemeris file makes it easy to compute the reflection point, as well as the extra-path delay for the reflected signal. A model is represented in Figure 11.

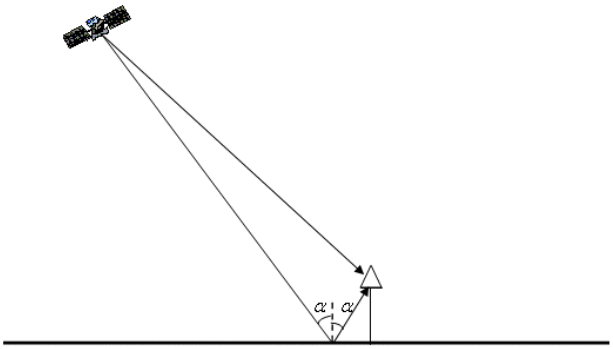

Figure 11 – Ground Reflection

Table 1 shows an example of the ground reflection delay for six GPS satellite in view with different elevations for an antenna 2 m above the ground.

Table 1 – Ground Reflection Delay for 6 Satellites in View and an Antenna 2 m Above the Ground

Satellite	1	2	4	13	16	20	25
Elev. (°)	64.1	39.1	20.1	32.6	45.3	57.2	37.8
Ground Refl. Delay (m)	4.33	5.98	11.3	6.32	5.48	3.68	2.87

The second kind of reflections simulated is coming from pre-defined obstacles. The user has the possibility to define any kind of object by inputting the coordinates of each corner and the surface reflection coefficient (fading in dB). The only constraint is for the object to be vertical. The computation of the satellite coordinates at all time and the knowledge of the antenna position allow determining if the direct signal is blocked, in which case, the obstacle's fading is applied to the direct signal. If the signal is not blocked, the program then searches for possible reflections against the obstacle. Finally, it also searches for a second reflection from the ground (path following satellite-obstacle-ground-antenna). Figure 12 shows an example of the method used.

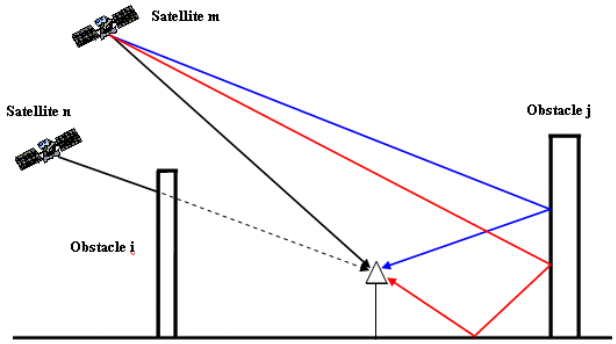

Figure 12 – Example of the Implementation of the Obstacle Reflection/Blocking

The algorithm can work with any number of obstacles. However, no multiple reflections were implemented.

Such a tool is very interesting to model specific environment. Moreover, it is possible to have blocking or fading from these obstacles according to the fading parameter chosen. Of course, very complex environments cannot be modeled due to the limitation in the models (vertical objects only, no multiple reflections, assumption of large and smooth obstacles), but it can still be used to simulate harsh environment, as well as blocking gaps.

In order to give an example of the far echo implementation, a test was set up and is shown in Figure 13. The user describes a 50 metre circle around a tall obstacle whose edges, in Easting and Northing coordinates are (30, 30) and (-30, -30). The obstacle height is 50 metres. The antenna height was set to 2 metres. The user starts its trajectory at (50, 0). The amplitude of the multipath reflected from the obstacle is half of that of the direct signal. The obstacle's fading parameter was set to 50 dB to make sure the signal was blocked. Only the GPS C/A signal was simulated.

The software receiver described by Ma et al (2004) was used to process the IF data. Seven channels were used to track each satellite. A Narrow Correlator (0.3 chips) DLL was used. The correct Doppler and code delays were input in the receiver. The PLL used was set with a large loop bandwidth (30 Hz) in order to ensure carrier tracking after short delay signal blocking (no re-acquisition procedure was used).

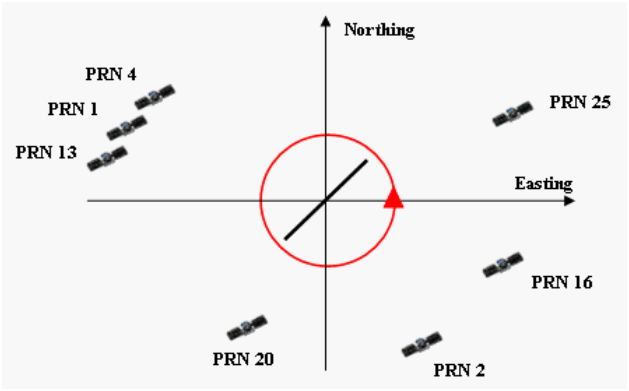

Figure 13 – Test 1 Configuration

Figure 14 shows the signal power for each of the seven satellites for the first 1.75 seconds of the scenario, representing the first quarter of the circle travelled by the user. All the satellite elevations are given in Table 1. The results agree well with the theory. Two examples are given hereafter:

- Satellite 1, thanks to its high elevation, can 'see' the receiver at the beginning, so tracking is possible. The user then gets closer to the obstacle, inducing a

masking that results in a loss of lock. The signal is reacquired shortly after, as the user passes beside the obstacle. Then, because the user is in front of the obstacle and fairly close to it, it will be subject to reflections that can be observed through the noisier $\sqrt{I^2+Q^2}$ values. Finally, because the obstacle is only 50 metre high, and the satellite is at high elevation, it cannot reflect the signal to the receiver, explaining the clean tracking.

- Satellite 20 can see the antenna at the beginning of the test and so is being properly tracked. Shortly after, as the user gets closer to the obstacle, a strong reflection appears and enters the receiver front end. When the user passes at the top right of the obstacle, no reflected signal occurs and cleaner tracking is possible until the user goes behind the obstacle. This causes masking and a loss of tracking. Finally, because satellite 20 is on the side of the obstacle, its signal can be re-acquired shortly after.

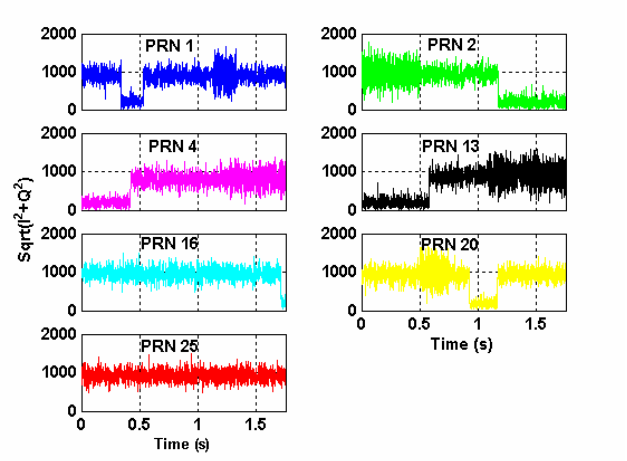

Figure 14 - $\sqrt{I^2+Q^2}$ for the Seven Satellites Simulated During the First 1.75 Seconds

In order to make the IF signal simulator more realistic, it is important as well to closely model the front end of the receiver. In this respect, the received signal power, as well as the antenna gain pattern is tremendously important.

Front End Design

The power level of the received signal is a function of the elevation angle. The GPS system was designed to have the highest received signal power for satellites being at 45 degree elevation. The same approach was adopted for the GNSS IF signal simulator. The received power, without any obstacles, is shown in Figure 15.

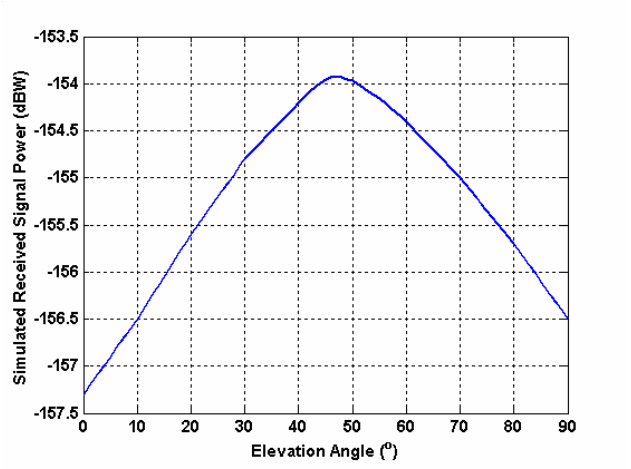

Figure 15 – Simulated Received Signal Power as a Function of the Elevation Angle

The difference in the received signal power between 45 and 90 degree elevation angle reaches approximately 2.5 dB, which cannot be neglected. This will be very important, especially when an antenna gain pattern is used.

Antenna Gain Pattern

The antenna gain pattern has a tremendous impact on the signal tracking. Different applications will use different antennas. A ship will use antenna with a significant gain at low elevation in order to be able to keep tracking low elevation satellites even in case of high roll. On the other hand, a geodetic antenna will have a very low gain at low elevation in order to reject the potential multipath coming from the ground. Four antenna gain patterns are implemented so far in the software GNSS IF signal generator: the first one is an isotropic antenna that has the same unit gain for all elevations and for both Right Hand Circularly Polarized (RHCP) and Left Hand Circularly Polarized (LHCP) signals. This antenna allows having no discrimination at the antenna level in case one wants to use all the possible signals with predetermined C/N_o, or in order to receive strong multipath from diverse angles without having them mitigated. The three other antennas were taken from the NovAtel family: the 501, 503, and 600 (NovAtel 2004). Both the RHCP and the LHCP gain patterns were implemented in order to be able to discriminate multipath with a change in its polarization. Of course, any antenna gain pattern can be implemented if other kinds of antennas are considered useful. Such a tool enables testing of diverse algorithms using different possible antennas to assess their impact on algorithm performance. An example could be the assessment of the importance of the antenna when a strong signal coming from a high elevation satellite, undergoing a high antenna gain, can affect the acquisition of a weaker low elevation satellite, with low antenna gain.

It can also be used to assess the impact of the antenna on multipath rejection, when combined with the multipath generation module of the software. As an example, a GPS C/A signal coming from a 65 degree elevation angle with a C/N_o of 50 dB-Hz was simulated, along with a long delay multipath (300 metres) with a power equal to half the power of the direct signal, coming from a low elevation (10 degrees). The four types of antenna were used, and an acquisition process, using a 5 ms coherent integration was started. Figure 16 shows the value of the $\sqrt{I^2+Q^2}$ during the acquisition process, assuming a correct Doppler estimate, and zooming in around the correct code delay. It can be observed that the choice of the antenna has a tremendous impact on mitigating the kind of multipath simulated. While the antenna with a uniform unit gain is very affected by the multipath (second peak 1 chip away from the direct signal), the other antennas succeed in mitigating the multipath, with different levels of success. Moreover, it is interesting to notice the difference in the gain as a function of satellite elevation (the y-axis is different for each figure).

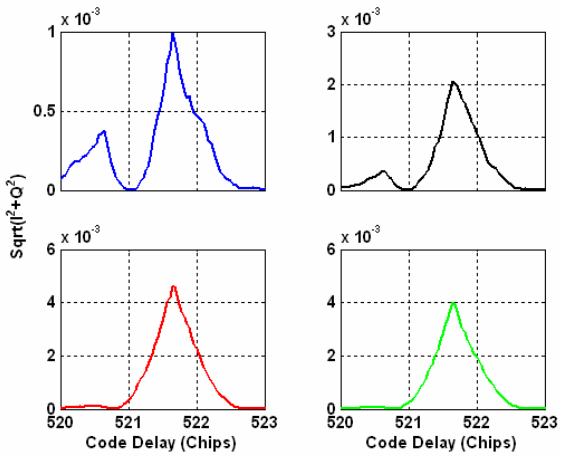

Figure 16 - $\sqrt{I^2+Q^2}$ During the Acquisition Process Using a Uniform Unit Gain Antenna (Top Left), a NovAtel GPS 501 Antenna (Top Right), A NovAtel GPS 503 Antenna (Bottom Left), and A NovAtel GPS 600 Antenna (Bottom Right) in Presence of a Strong Multipath Coming from a 10 Degree Elevation

CONCLUSIONS

The development of a software IF GNSS signal generator by the PLAN Group of the University of Calgary has resulted in an advanced tool that allows for a diversity of research applications. It includes the modelling of all the major sources of errors affecting GNSS signal reception such as satellite clock errors, atmospheric effects, multipath, and thermal noise. The enhancement brought by the implementation of a realistic received power gain pattern and several antenna gain patterns makes this IF signal generator very useful to simulate simple to complex real environments.

The object-oriented implementation makes the addition of more advanced modules, such as the generation of more signals, or a new version of the multipath generation module, very simple.

Through the many studies realised at the University of Calgary, this software IF GNSS signal generator has already proven to be very effective in the development of a software receiver thanks to its high flexibility. It is also being used extensively for the development of GPS II and Galileo tracking techniques. Finally, it is an efficient tool to test new software receiver-based algorithms in real environment without the need for a hardware signal simulator for a variety of tasks, ranging from interference to indoor tracking.

ACKNOWLEDGEMENT

The authors acknowledge the Alberta Ingenuity Fund and Alberta's Informatic Centre Of Research Excellence (iCORE) for its financial support.

REFERENCES

Alves, P. (2001), The effect of Galileo on Carrier Phase Ambiguity Resolution, Proceedings of the US Institute of Navigation GPS (Salt Lake City, UT, USA, Sept. 11-14), pp. 2086-2095.

Bastide F., O. Julien, C. Macabiau, and B. Roturier (2002), *Analysis of L5/E5 Acquisition, Tracking and Data Demodulation Thresholds*, Proceedings of the US Institute of Navigation GPS (Portland, OR, USA, Sept. 24-27), pp. 2196-2207.

Brenner, M., R. Reuters, and B. Schipper (1998), *GPS Landing System Multipath Evaluation Techniques and Results*, Proceedings of the US Institute of Navigation GPS (Nashville, TN, USA, Sept. 15-18), pp. 999-1008.

Dong, L., C. Ma, and G. Lachapelle (2004), *Implementation and Verification of a Software-Based IF GPS Signal Simulator*, Proceedings of the US Institute of Navigation National Technical Meeting (San Diego, Jan 26-28), pp.378-389.

Dong, L. (2003) *IF GPS Signal Simulator Development and Verification*, M.Sc. Thesis, UCGE 20184, (URL: http://www.geomatics.ucalgary.ca/links/GradTheses.html)

Döttling M., A. Jahn, D. Didascalou, and W Wiesbeck (2001), *Two- and Three-Dimensional Ray Tracing Applied to the Land Mobile Satellite (LMS) Propagation*

Channel, IEEE Antennas and Propagation Magazine, Vol. 43, No. 6, Dec., pp. 27-37.

Hegarty, C., M. Tran, and A.J. Van Dierendonck (2003), *Acquisition Algorithms for GPS L5*, CD-ROM Proceedings of the European Navigation Conference GNSS, (Graz, Austria, April 22-), 14 pages.

Hegarty, C., M. Tran, and J. Betz (2004), *Multipath performance of the New GNSS Signals*, Proceeding of the US Institute of Navigation NTM (San Diego, CA< USA, Jan. 26-28), pp. 333-342.

Jahn, A., H. Bischl, G. Heiss (1996), *Channel Characterisation for Spread Spectrum Satellite Communication*, Spread, IEEE 4th International Symposium on Spectrum Techniques and Applications Proceedings, Vol. 3, (Sept. 22-25), pp. 1221-1226.

Julien, O., P. Alves, M.E. Cannon, and G. Lachapelle (2004a) *Improved Triple-Frequency GPS/Galileo Carrier Phase Ambiguity Resolution Using a Stochastic Ionosphere Modeling*, Proceedings of the US Institute of Navigation NTM (San Diego, CA, USA, Jan. 24-28), 441-452.

Julien, O., M.E. Cannon, P. Alves, and G. Lachapelle (2004b), *Triple Frequency Ambiguity Resolution Using GPS/Galileo*. European Journal of Navigation, Vol. 2, Number 2, pp. 51-57.

Kuusniemi, H., G. Lachapelle, and J. Takala (2004), *Reliability in Personal Positioning*, CD-ROM Proceedings of the European Navigation Conference GNSS, (Rotterdam, The Netherlands, May 16-19), Session 'Land-Based Applications I', 12 pages.

Ma, C., G. Jee, G. MacGougan, G. Lachapelle, S. Bloebaum, G. Cox, L. Garin and J. Shewfelt (2001) *GPS Signal Degradation Modeling*, Proceedings of the US Institute of Navigation GPS, (Session C2, Salt Lake City, UT, USA, September 11-14), pp. 882-893.

Ma, C., G, Lachapelle, and M.E. Cannon (2004) *Implementation of a Software GPS Receiver*, Proceedings of the US Institute of Navigation GNSS (Long Beach, CA, USA, Sept. 22-25).

Macabiau, C., L. Ries, F. Bastide, and J.-L. Issler (2003), *GPS L5 Receiver Implementation Issues*, Proceedings of the US Institute of Navigtion GPS/GNSS (Portland, OR, USA, Sept. 9-12), pp. 153-164.

NovAtel (2004), http://www.novatel.ca

Steingass, A., A. Lehner, F. Pérez-Fontán, E. Kubista, M.J. Martín, and B. Arbesser-Rastburg (2004), *The High Resolution Aeronautical Multipath Navigation Channel*, Proceedings of US Institute of Navigation NTM (San Diego, CA, USA, Jan. 24-28), pp. 793-804.

Spilker, J. J. and A. J. Van Dierendonck (2001), *Proposed New L5 Civil GPS Codes*, Navigation: Journal of The Institute of Navigation, Vol.48, No.3, Fall.

Tran, M, and C. Hegarty (2002), Receiver Algorithms for the New Civil GPS Signals, Proceedings of the US Institute of Navigation NTM (San Diego, CA, USA, Jan. 28-30), pp. 778-789.

Zheng, B., and G. Lachapelle (2004), *Acquisition Schemes for a GPS L5 Software Receiver*, Proceedings of the ION GNSS (Long Beach, CA, USA,Sept. 21-24).

Winkel, J.O. (2003), *Modeling and Simulating GNSS Signal Structures and Receivers*, PhD dissertation, Thesis, University FAF Munich, Neubiberg.